Research Article | Vol. 10, No. 10 / 1 October 2019 / Biomedical Optics Express 5025
Biomedical Optics EXPRESS

Polar organization of collagen in human cardiac tissue revealed with polarimetric second-harmonic generation microscopy

KAMDIN MIRSANAYE,[1,2] AHMAD GOLARAEI,[1,2,3] FAYEZ HABACH,[2] EDVARDAS ŽURAUSKAS,[4] JONAS VENIUS,[5,6] RICARDAS ROTOMSKIS,[5,7] AND VIRGINIJUS BARZDA[1,2,7,*]

[1]*Department of Physics, University of Toronto, 60 St. George St, Toronto, M5S 1A7, Canada*
[2]*Department of Chemical and Physical Sciences, University of Toronto Mississauga, 3359 Mississauga Rd North, Mississauga, L5L 1C6, Canada*
[3]*Princess Margaret Cancer Centre, University Health Network, 101 College St, Toronto, M5G 1L7, Canada*
[4]*Department of Pathology, Forensic Medicine and Pharmacology, Faculty of Medicine, Vilnius University, M.K. Ciurlionio St 21/27, LT-03101, Vilnius, Lithuania*
[5]*Biomedical Physics Laboratory, National Cancer Institute, P. Baublio St 3b, LT-08406, Vilnius, Lithuania*
[6]*Medical Physics Department, National Cancer Institute, Santariskiu St 1, LT-08660, Vilnius, Lithuania*
[7]*Laser Research Center, Vilnius University, Sauletekio Ave 9 corp. III, LT-10222, Vilnius, Lithuania*
[*]*virgis.barzda@utoronto.ca*

Abstract: Polarimetric second-harmonic generation (P-SHG) microscopy is used to characterize the composition and polarity of collagen fibers in various regions of human cardiac tissue. The boundary between the cardiac conduction system and myocardium is shown to possess a distinct composition of collagen compared to other regions in the heart. Moreover, collagen fibers in this region are macroscopically organized in a unipolar arrangement, which may consequently aid in effective propagation of the electrical signal through the cardiac conduction system.

1. Introduction

The cardiac conduction system (CCS) is a collection of specialized cells, responsible for generating and guiding electrical signals within the heart, ensuring coherent contractions of the cardiac muscles, and efficient pumping of blood in the body [1]. One of the main constituents of the heart tissue is collagen, which is comprised of polar molecules [2] with helical structures [3]. Collagen has been previously shown to isolate the CCS from the rest of the cardiac tissue, resulting in effective transduction of the electrical signal [4,5]. However, the exact differences in organization of collagen surrounding the CCS are not very well understood.

Collagen can be readily visualized using second-harmonic generation (SHG) microscopy [6], due to its noncentrosymmetric structure. Furthermore, polarization-resolved SHG (P-SHG) microscopy can be utilized to investigate the composition and three-dimensional organization of collagen, through the extraction of two second-order nonlinear susceptibility tensor element ratios, as well as the in-image-plane collagen fiber orientation angle [7]. The achiral susceptibility ratio (R-ratio) has been previously used to differentiate between tissue types [8], as well as, normal and malignant tissues in various organs [9–11]. Moreover, the chiral susceptibility ratio (C-ratio) has been introduced recently to study the polarity of collagen fibers [7].

It is well established that collagen exhibits shear piezoelectricity [12–14]. Most mechanical properties of collagen polarity and piezoelectricity have been studied in tissue [15,16]. However, the role of collagen polarity in efficient conduction of electrical signals in the CCS remains unknown. In this work, P-SHG is used to study collagen ultrastructure in several regions of the cardiac tissue, ultimately providing evidence for the unipolar arrangement of collagen in the CCS.

#367915 https://doi.org/10.1364/BOE.10.005025
Journal © 2019 Received 20 May 2019; revised 16 Aug 2019; accepted 16 Aug 2019; published 10 Sep 2019

Biomedical Optics EXPRESS

2. Materials and methods

2.1. Polarization-in, polarization-out (PIPO) microscopy

To probe the ultrastructural properties of the collagen fibers, linear polarization-in, polarization-out (PIPO) analysis is carried out [8]. A molecular coordinate system, pertaining to collagen fibers within each focal volume, is denoted by the lower case indices *xyz*. The arbitrarily oriented molecular coordinate system is related to the laboratory coordinate system, *XYZ* (see Fig. 1(e)), via the in-image-plane (*XZ*-plane) orientation angle (δ), and the out-of-plane tilt angle (α). The beam propagation direction is along the *Y*-axis, and the polarizer and analyzer orientation angles, are denoted by θ and ϕ, respectively. Far from sample absorption, real-valued susceptibility components are considered. In addition, due to the presence of dominant $\chi^{(2)}_{zzz}$, $\chi^{(2)}_{xxz}/\chi^{(2)}_{zxx} = 1$ is assumed [17]. Neglecting birefringence in thin (4 μm) sample thickness and assuming C_6 symmetry for collagen fibers, the P-SHG intensity relation can be written as in Eq. (1) [7]:

$$I_{2\omega} \propto \Big| \sin(\phi-\delta)\sin(2\theta-2\delta) + 2\mathrm{C}\cos(\theta-\delta)\sin(\theta-\phi) + \cos(\phi-\delta)\sin^2(\theta-\delta) + \mathrm{R}\cos(\phi-\delta)\cos^2(\theta-\delta)\Big|^2 \tag{1}$$

where C and R are susceptibility element ratios, as defined in Eq. (2) [7].

$$\mathrm{C} = \frac{\chi^{(2)}_{xyz}}{\chi^{(2)}_{zxx}}\sin(\alpha), \qquad \mathrm{R} = \frac{\chi^{(2)}_{zzz}}{\chi^{(2)}_{zxx}}\cos^2(\alpha) + 3\sin^2(\alpha) \tag{2}$$

The R-ratio is most sensitive to the molecular composition of the underlying tissue, while also varying with the fiber orientation. The C-ratio is predominantly sensitive to the polarity and the out-of-plane orientation of the collagen fibers [7].

2.2. Experimental setup

A custom-built polarimetric nonlinear laser scanning microscope was used for P-SHG imaging of cardiac tissue [8]. The laser source consisted of a home-made diode-pumped Yb:KGW oscillator (1028 nm emission wavelength, 430 fs pulse duration, and 14.3 MHz pulse repetition rate) [19]. The incident linear polarization is set using a nano-particle glass linear polarizer (colorPol IR 1100 BC4, Laser Components Inc.) and a half-wave plate (532GR42, Comar Optics). The beam is focused onto the sample by an air objective (20X, 0.75 NA, Carl Zeiss), and the SHG signal is collected by a custom objective (0.85 NA) and a linear polarizer (colorPol VIS 500 BC4, Laser Components Inc.). The half-wave plate and analyzer were rotated by a motorized rotation mounts (PRM1Z8, Thorlabs). The SHG signal is filtered by a Schott glass BG39 and a 510 – 20 nm band-pass filter (Edmund Optics), and detected by a photon counting photomultiplier tube (Hamamatsu H7421-40).

To perform PIPO polarimetry, a set of 9 equally spaced incident linear polarization states between 0 and π is prepared. For each incident state, a set of 9 outgoing polarization states of the SHG signal is measured [8]. The acquisition time for each polarization state is 7 seconds, the total measurement time including polarizer rotation time is about 25 min. The P-SHG intensity is fitted with Eq. (1) at each pixel with a custom trust-reflective region fitting algorithm [18], with a minimum goodness of fit $R^2 = 0.95$ for statistical considerations. The C-ratio, R-ratio, and δ are extracted as fit parameters.

2.3. Sample preparation

The human heart tissue samples were obtained during autopsies, no later than 48 hours after death, according to institutionally-approved protocols (National Centre of Pathology, Vilnius,

Biomedical Optics EXPRESS

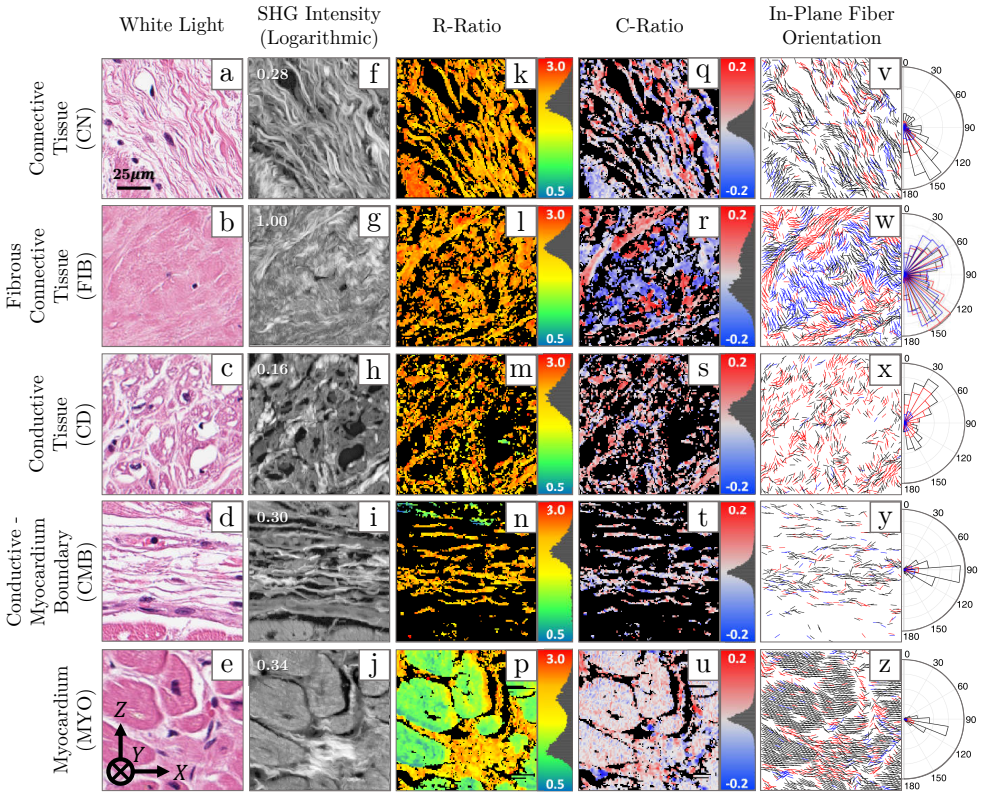

Fig. 1. Representative images from CN, FIB, CD, CMB and MYO regions of the human cardiac tissue. H&E images (a)-(e), total SHG intensity on a logarithmic scale (f)-(j), R- and C-ratios (k)-(p) and (q)-(u), respectively (the occurrence histograms are embedded in their color bars), the in-plane orientation (δ) of the collagen fibers (v)-(z) and their corresponding polar distribution (red and blue lines indicate positive and negative polarities, respectively, the black lines show the fibers in the image plane with $|C| \leq 0.03$). Imaged areas were 110 μm × 110 μm (128 × 128 pixels). Pixels with fewer than 20 photon counts for every polarization state are discarded in analysis. Minimum goodness of fit is $R^2 = 0.8$.

Lithuania). Tissues were fixed in 10% buffered formalin solution. Sections of 4 μm thickness were prepared with the Leica RM2145 microtome and stained by hematoxylin and eosin (H&E) stain, for visualization with white light microscope. Collagen-containing areas of interest were selected by a pathologist (E. Ž.) for P-SHG imaging.

3. Results and discussion

Five different collagen-containing regions of the heart, including various connective tissues (CN), densely packed fibrous body (FIB), conductive tissue of the CCS, including His bundle and bundle branches (CD), the boundary between the CCS and the adjacent myocardium (CMB), and the interior of myocardium (MYO) were studied using P-SHG microscopy. A total of 56 areas of CN, 31 areas of FIB, 33 areas of CD, 36 areas of CMB, and 35 areas of MYO from 5 histology slides were scanned and analyzed. Figure 1 shows representative snapshots from each region. Figures 1(a)–1(e) present the white light images of the tissues, stained with H&E. Figures 1(f)–1(j) show the combined SHG intensity of all measured polarization states in the image, on a logarithmic scale (normalization on the top left). R- and C-ratios are shown in

Biomedical Optics EXPRESS

Figs. 1(k)–1(p) and Figs. 1(q)–1(u), respectively, and their histograms are embedded in each corresponding color bar. Lastly, Figs. 1(v)–1(z) illustrate the in-plane fiber orientation (δ), and their corresponding polar distribution. Fibers with positive and negative polarities are denoted by red and blue lines, respectively. The black lines indicate fibers that are approximately in the image plane.

The R-ratio clearly differentiates muscle (blue-green) and collagen (yellow-orange), which lie between $0.5 - 3$ and $1.5 - 3$, respectively (See Fig. 1(p)). The results are in agreement with previous studies of muscle [20] and collagen [21]. R-ratios of collagen appear slightly lower in CMB and MYO images, as indicated by more yellow pixels in Figs. 1(n) and 1(p).

According to Eq. (2), C-ratio varies with the sine of tilt angle α, resulting in blue and red pixels depending on the positive or negative fiber orientation out of the image plane. It has been shown that bimodal, positive and negative, distribution of C-ratio corresponds to the bipolar arrangement of collagen fibers in the pig tendon tissue [7]. Although both positive and negative C-ratio values of collagen fibers have been observed in all 5 regions, FIB areas showed a bimodal distribution and a significantly larger overall standard deviation of the C-ratio (see Fig. 1(r)). In addition, 6 imaged areas surrounding blood vessels in CN showed similar bimodal C-ratio distributions (data not shown). As a result, it can be concluded that these areas possess significant bipolar arrangement of collagen. In contrast, the CMB shows a relatively narrow distribution of C-ratio around zero, suggesting smaller fiber angle variations and unipolar arrangement of collagen. The C-ratio distributions of CD, and MYO were slightly wider than CMB, however, bimodal C-ratio distributions were not observed, also suggesting a unipolar arrangement of collagen fibers with larger orientation spread in these regions. Moreover, it is evident that CN, and CMB (Figs. 1(v) and 1(y)) have a higher degree of in-plane fiber alignment, while collagen fibers in CD and FIB (Figs. 1(x) and 1(w)) are more disorganized.

The observed differences in collagen organization between all regions were further investigated via statistical comparisons of all analyzed scans, using MATLAB's built-in functions. The R-ratio and C-ratio of all imaged regions have been considered, and the mean, and standard deviation of the resulting distributions were calculated and compared. Otsu's thresholding method has been used to separate muscle and collagen data, according to their significant R-ratio value differences (see Fig. 2(a)) [22]. R-ratio values larger than $R = 1.55$ are used to represent collgeneous tissue. Following the truncation, R- and C-ratio distributions of each data set were first tested for normality using Shapiro-Wilk test, which indicated that most data sets were not exhibiting normal distributions. As a result, Kruskal-Willis combined with Bonferroni multiple comparisons tests were performed to examine statistical significance of the differences between the regions.

R-ratio mean (μ_R) is sensitive to the ultrastructural organization of the underlying tissue. Therefore, statistical considerations of μ_R are predominantly helpful in distinguishing subtle variations in the material ultrastructure. Figure 2(b) shows that CMB possesses a statistically significant lower μ_R compared to each of CN, FIB, and CD (p-values of 0.028, 0.047, 0.044, respectively). Similarly, MYO shows a highly significant lower μ_R compared to each of CN, FIB and CD (p-values <0.0001), while no statistically significant differences were observed between μ_R of CN, FIB and CD. In addition, μ_R of MYO was slightly lower than CMB, however, not significantly different. The R-ratio results show that CN, FIB and CD regions have very similar collagen ultrastructural organization, while collage in CMB and MYO is significantly different from the aforementioned regions.

The C-ratio values are very sensitive to the tilt angle α. Since tissue sections were cut at random orientations, the standard deviation of C-ratio distribution (σ_C) was chosen for the statistical analysis, instead of the mean of C-ratio. The σ_C parameter was utilized to investigate the bipolar arrangements of collagen fibers in each region. The σ_C results indicate a clearly significant difference between FIB and all other regions, with the smallest difference of 0.013

Biomedical Optics EXPRESS

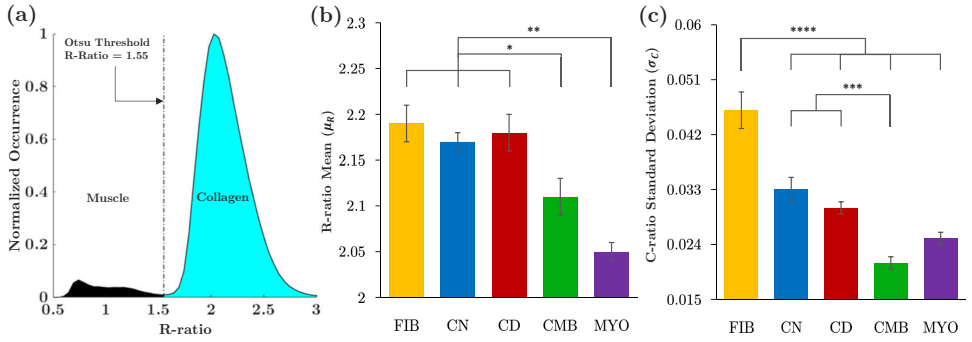

Fig. 2. Statistical analysis of R- and C-ratios. The R-ratio distribution from all analyzed images combined, with myosin (black) and collagen (cyan) R-ratios separated by Otsu's threshold at 1.55 (a). R-ratio mean (b) and C-ratio standard deviation (c) of all scanned regions of the human cardiac tissue. Standard errors are represented by error bars, and asterisks denote statistical significance: $*\ p<0.05$, $**\ p<0.0001$, $***\ p<0.001$, $****\ p<0.02$.

between FIB and CN (p-value of 0.016). CMB also shows highly significantly different σ_C, compared to CN, CD, and FIB (p-values <0.001), as shown in Fig. 2(c). These results provide quantitative evidence that CMB shows no clear signs of bipolar collagen arrangements (lower σ_C), while in contrast, FIB, as well as 6 CN areas near blood vessels show prominent signs of bipolarity (larger σ_C). Further investigations are needed to determine the polar arrangement of collagen fibrils at the nano-scale within the focal volumes, however the high degree of unipolar arrangement at the macroscopic tissue level is evident from the P-SHG microscopy data.

Unipolar or bipolar arrangement of collagen fibers may alter the bulk piezoelectric properties of collagen-containing tissues, resulting in facilitation, or hindrance of the unidirectional electrical signal propagation, respectively. More specifically, unipolar organization of collagen in CMB, CD and MYO may play an important role in the unidirectional propagation of electrical signal in the heart. On the other hand, bipolar arrangement of collagen fibers in FIB and around the blood vessels may minimize the effects of bulk piezoelectricity, resulting in the insulating nature of the collagenous tissue in these regions.

4. Conclusion

P-SHG measurements reveal specific differences in several collagen-containing regions of the heart. At the ultrastructural level, the R-ratio shows that connective tissue, fibrous body and conductive tissue possess similar collagen organization. Moreover, the C-ratio illustrates a bipolar arrangement of collagen in the fibrous body and around blood vessels at the macroscopic scale. This suggests that bipolar organization of collagen reduces bulk piezoelectric effect, giving rise to electrically insulating properties of collagen in these regions. The collagenous boundary layer between conductive tissue and myocardium (CMB) shows different R-ratio mean values, compared to the connective and conductive tissues. In addition, narrow C-ratio distribution suggests unipolar arrangement of collagen in this region. The unipolar collagen organization in CMB may play an important physiological role in facilitating fast unidirectional propagation of electrical signal in the cardiac conduction system. The unipolar collagen organization is also observed inside the conductive system and myocardium, albeit with larger spread of C-ratio values compared to CMB. Therefore, varied distributions of collagen fiber orientations could influence the speed of electrical signal propagation in different regions of the heart.

Biomedical Optics EXPRESS

Funding

Natural Sciences and Engineering Research Council of Canada (CHRPJ 462842-14, DGDND-2017-0009906923, RGPIN-2017-06923); Canadian Institutes of Health Research (CPG-134752); European Regional Development Fund; Research Council of Lithuania (No. 1.2.2.-LMT-K-718-02-0016).

Acknowledgments

We would like to thank Leonardo José Uribe Castaño for help with the laser system.

Disclosures

The authors declare that there are no conflicts of interest related to this article.

References

1. F. Martini, R. B. Tallitsch, and J. L. Nath, *Human Anatomy* (Pearson, 2017).
2. D. A. D. Parry and A. S. Craig, "Collagen structure and stability," Biopolymers **16**(5), 1015–1031 (1977).
3. G. N. Ramachandran and G. Kartha, "Structure of Collagen," Nature **176**(4482), 593–595 (1955).
4. J. Venius, E. Zurauskas, and R. Rotomskis, "High Resolution Imaging of the Human Cardiac Conduction System Using Reflectance Confocal Microscopy," Tohoku J. Exp. Med. **229**(1), 67–73 (2013).
5. J. Venius, S. Bagdonas, E. Zurauskas, and R. Rotomskis, "Visualization of human heart conduction system by means of fluorescence spectroscopy," J. Biomed. Opt. **16**(10), 107001 (2011).
6. I. Freund and M. Deutsch, "Macroscopic polarity of connective tissue is due to discrete polar structures," Biopolymers **25**(4), 601–606 (1986).
7. A. Golaraei, K. Mirsanaye, Y. Ro, S. Krouglov, M. K. Akens, B. C. Wilson, and V. Barzda, "Collagen chirality and 3D orientation studied with polarimetric second-harmonic generation microscopy," J. Biophotonics **12**(1), e201800241 (2019).
8. A. E. Tuer, M. K. Akens, S. Krouglov, D. Sandkuijl, B. C. Wilson, C. M. Whyne, and V. Barzda, "Hierarchical Model of Fibrillar Collagen Organization for Interpreting the Second-Order Susceptibility Tensors in Biological Tissue," Biophys. J. **103**(10), 2093–2105 (2012).
9. A. Golaraei, R. Cisek, S. Krouglov, R. Navab, C. Niu, S. Sakashita, K. Yasufuku, M. Tsao, B. C. Wilson, and V. Barzda, "Characterization of collagen in non-small cell lung carcinoma with second harmonic polarization microscopy," Biomed. Opt. Express **5**(10), 3562–3567 (2014).
10. A. Golaraei, L. Kontenis, R. Cisek, D. Tokarz, S. J. Done, B. C. Wilson, and V. Barzda, "Changes of collagen ultrastructure in breast cancer tissue determined by second-harmonic generation double Stokes-Mueller polarimetric microscopy," Biomed. Opt. Express **7**(10), 4054–4068 (2016).
11. D. Tokarz, R. Cisek, A. Joseph, A. Golaraei, K. Mirsanaye, S. Krouglov, S. L. Asa, B. C. Wilson, and V. Barzda, "Characterization of Pancreatic Cancer Tissue Using Multiphoton Excitation Fluorescence and Polarization-Sensitive Harmonic Generation Microscopy," Front. Oncol. **9**, 272 (2019).
12. E. Fukada and I. Yasuda, "On the piezoelectric effect of bone," J. Phys. Soc. Jpn. **12**(10), 1158–1162 (1957).
13. E. Fukada and I. Yasuda, "Piezoelectric effects in collagen," Jpn. J. Appl. Phys. **3**(2), 117–121 (1964).
14. M. H. Shamos and L. S. Lavine, "Piezoelectricity as a fundamental property of biological tissues," Nature **213**(5073), 267–269 (1967).
15. M. Minary-Jolandan and M. Yu, "Nanoscale characterization of isolated individual type I collagen fibrils: Polarization and piezoelectricity," Nanotechnology **20**(8), 085706 (2009).
16. C. P. Brown, J. L. Boyd, A. J. Palmer, M. Phillips, C. Couture, M. Rivard, P. A. Hulley, A. J. Price, A. Ruediger, F. Légaré, and A. J. Carr, "Modulation of Mechanical Interactions by Local Piezoelectric Effects," Adv. Funct. Mater. **26**(42), 7662–7667 (2016).
17. C. A. Dailey, B. J. Burke, and G. J. Simpson, "The general failure of Kleinman symmetry in practical nonlinear optical applications," Chem. Phys. Lett. **390**(1-3), 8–13 (2004).
18. T. F. Coleman and Y. Li, "An Interior, Trust Region Approach for Nonlinear Minimization Subject to Bounds," SIAM J. Optim. **6**(2), 418–445 (1996).
19. A. Major, R. Cisek, and V. Barzda, "Femtosecond Yb:KGd$(WO_4)_2$ laser oscillator pumped by a high power fiber-coupled diode laser module," Opt. Express **14**(25), 12163–12168 (2006).
20. S. V. Plotnikov, A. C. Millard, P. J. Campagnola, and W. A. Mohler, "Characterization of the myosin-based source for second-harmonic generation from muscle sarcomeres," Biophys. J. **90**(2), 693–703 (2006).
21. X. Chen, O. Nadiarynkh, S. Plotnikov, and P. J. Campagnola, "Second harmonic generation microscopy for quantitative analysis of collagen fibrillar structure," Nat. Protoc. **7**(4), 654–669 (2012).
22. N. Otsu, "A Threshold Selection Method from Gray-Level Histograms," IEEE Trans. Syst., Man, Cybern. **9**(1), 62–66 (1979).